A table of contents entry

Novel Hg^{2+} ion-imprinted polymers were synthesized using the chelate of dithizone and Hg^{2+} as template, for mercury speciation analysis.

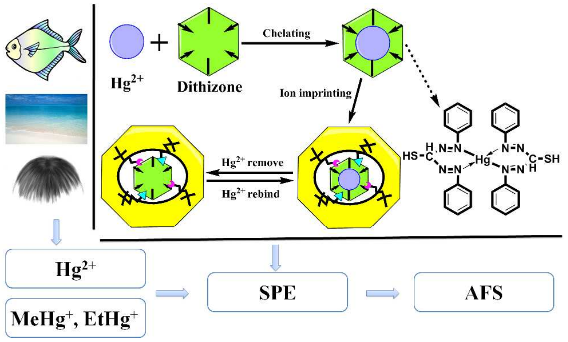

Cite this: DOI: 10.1039/c0xx00000x

www.rsc.org/xxxxxx

ARTICLE TYPE

Hg^{2+} ion-imprinted polymers sorbents based on dithizone-Hg^{2+} chelation for mercury speciation analysis in environmental and biological samples

Zhong Zhang,[a,d] Jinhua Li,[a] Xingliang Song,[b] Jiping Ma[c] and Lingxin Chen*[a]

Received (in XXX, XXX) Xth XXXXXXXXX 20XX, Accepted Xth XXXXXXXXX 20XX

DOI: 10.1039/b000000x

Novel Hg^{2+} ion-imprinted polymers (IIPs) were synthesized by sol–gel process, using the chelate of dithizone and Hg^{2+} as template and 3-aminopropyltriethoxysilane as functional monomer, followed by solid-phase extraction (SPE) and atomic fluorescence spectroscopy (AFS) detection, for mercury speciation analysis in environmental and biological samples. The resultant Hg-IIPs offered high binding capacity, fast kinetics, and the adsorption processes followed Langmuir isotherm and pseudo-second-order kinetic models. The IIPs displayed excellent selectivity toward Hg^{2+} over its organic forms and other metal ions with selectivity factors of 19–34, as well as high anti-interference ability for Hg^{2+} confronting with common coexistent ions. Through 10 adsorption-desorption cycles, the IIPs showed a good reusability with the relative standard deviations within 5%. Moreover, by virtue of the chelation of dithizone, the IIPs could readily discriminate Hg^{2+} from organic mercury. So, mercury speciation analysis could be attained, presenting high detectability up to 0.015 μg/L for Hg^{2+} and 0.02 μg/L for organic mercury, by using IIPs-SPE-AFS. The method was validated by using two certified reference materials with very consistent results. Satisfactory recoveries ranging from 93.0–105.2% were attained for spiked seawater and lake water samples with three concentration levels Hg^{2+}. Furthermore, the analytical results for the spiked mercury species in real biological samples such as human hair and fish meat, proved the methods practically applicable to speciation analysis. The IIPs-SPE-AFS demonstrated great application perspectives for rapid and high-effective cleanup, enrichment and determination of trace mercury species in complicated matrices.

1. Introduction

Heavy metals have received wide international concerns owing to their difficult degradation and high bioaccumulation properties, and thereby severe environmental/ecotoxicological threats.[1–4] Among them, mercury (Hg) has become a research hotspot,[1–6] and it has negative impact on humans usually through food especially fish.[7,8] Its toxicity depends on its chemical forms, and organic mercury compounds generally are much higher toxic than inorganic mercury, owing to their strong lipophilic characteristics.[7–10] Hence, speciation analysis of mercury ion (Hg^{2+}) and its organic species is increasingly investigated, since the monitoring and remediation of heavy metal pollution has become a crucial global issue. The separation and determination of mercury species is generally performed using chromatographic techniques, such as gas chromatography (GC), liquid chromatography (LC), ion chromatography (IC) and capillary electrophoresis (CE) for separation,[5,6,8,11] often coupled with element selective detectors, *e.g.* inductively coupled plasma mass spectrometry (ICP-MS),[12] atomic absorption spectroscopy (AAS),[13] and atomic fluorescence spectroscopy (AFS).[14–16] However, these instrument techniques are usually rather complex, costly, and time-consuming. On the other hand, the trace/ultra-trace presence of targeted analytes in complicated matrices has become the bottleneck of actual application analysis.[17] So, it is quite important to develop high-efficiency pretreatment and enrichment techniques/processes almost indispensable. Amongst them, solid-phase extraction (SPE) with selective sorbents gains great popularity.[18,19]

Ion-imprinted polymers (IIPs), a branch of molecularly imprinted polymers (MIPs), have aroused great interest as selective SPE sorbents for a particular chemical form of a given element.[4,20–24] IIPs are similar to MIPs, but they recognize inorganic ions after imprinting, especially metal ions.[20,21,24–27] The recognition ability can be explained by the polymer's memory effects toward the metal ion interaction with a specific ligand, coordination geometry, metal ion coordination number, charge and size.[28] The metal IIPs have attracted increasing attentions owing to their unique features: first, the coordination reaction is stronger than hydrogen bond strength, especially in aqueous solution; second, it is quite quick to achieve the balance of the thermodynamics and kinetics.[29,30] A number of studies on IIPs and their applications for selective preconcentration and separation of metal ions have been reported lately.[20,21,28,30,31] However, the IIPs related researches are often confronted with the challenges of incomplete ion removal and low selectivity, since many metal ions have the same charges, similar ionic radius and properties.[28,32,33] In order to overcome these weaknesses effectively, grafting method on the surface of polymer/silica gel beads, and utilizing selective ligands and/or functional monomers, for ion imprinting, have been developed.[33–35] For example, Dakova *et al.* prepared Hg(II) layer-coated silica gel particles (Hg(II)-IIP) for speciation and determination of mercury in wine.[34] Yan *et al.* proposed IIPs mesoporous materials for Zn^{2+} and Cd^{2+} detection, offering an alternative means of immobilizing small molecules.[35] Chen *et al.* synthesized specific ligand 3-isocyanatopropyltriethoxysilane and thereafter specific functional monomer, for specially imprinting Hg^{2+}, and attained highly selective preconcentration of Hg^{2+} in water samples.[33]

Dithizone, a well-known traditional ligand chelating agent for metal ions, with excellent selectivity advantages, has been increasingly used for mercury.[36–38] For instance, Liu and his coworkers developed a dithizone-functionalized SPE procedure followed by HPLC-ICP-MS for mercury in water samples.[37] Talpur *et al.* used surfactant coated alumina modified by dithizone for preconcentration and determination of trace amounts of mercury coupled with cold vapor AAS.[38] On the other hand, sol–gel technology, an easy-to-handle and ecofriendly strategy, has flourished for the synthesis of IIPs and MIPs.[33,39–41] However, as far as we are aware, no work combining IIPs, dithizone-Hg^{2+} chelate and sol–gel for mercury speciation analysis has been reported.

Inspired by these studies, herein, we proposed to synthesize novel Hg^{2+} imprinted IIPs by sol–gel process, using dithizone-Hg^{2+} chelate as template and 3-aminopropyltriethoxysilane as functional monomer, for mercury speciation analysis in environmental and biological samples, *via* selective SPE coupled with AFS detection. The selectivity of Hg-IIPs for Hg^{2+} *versus* other interfering metal ions (Zn^{2+}, Cd^{2+}, Pb^{2+}) and organic mercury species ($MeHg^+$, $EtHg^+$) was investigated. Two certified reference materials were utilized for validation, and the developed method was successfully applied for Hg^{2+} determination in environmental water samples, as well as organic mercury species determination in human hair and fish meat samples with satisfactory results.

2. Experimental

2.1. Reagents and materials

Mercury chloride ($HgCl_2$) and methylmercury (MeHg) chloride, as well as ethylmercury chloride (EtHg) standard solution (60 mg/L) were purchased from the CRM/RM Information Center of China (Beijing, China). Dithzone, 3-aminopropyltriethoxysilane (APTES) and tetraethoxysilicane (TEOS) were obtained from Sigma-Aldrich (Shanghai, China). Other affiliated reagents and materials were all supplied by Sinopharm Chemical Reagent (Shanghai, China). All the reagents were at least analytical grade and used directly without further purification unless otherwise specified. Aqueous solutions throughout the work were prepared using doubly purified deionized (DDI) water, which was produced by a Milli-Q Ultrapure water system with the water outlet operating at 18.2 MΩ (Millipore, MA, USA); all pH measurements were carried out by using a pHs-3TC digital pH meter equipped with a combined glass-calomel electrode (Shanghai, China).

2.2. Instrumentation

Atomic fluorescence measurements of mercury species were carried out with an AFS-3000 double-channel nondispersive atomic fluorescence spectrometer (Beijing Kechuang Haiguang Instrument Co., China). ICP-MS analyses were performed on PerkinElmer Elan DRC II (USA). FT-IR spectrometer (Nicolet iS10, Thermo scientific) was employed to record the infrared spectra of samples using a pressed KBr tablet method. Scanning electron microscope (SEM, Hitachi S-4800, Japan) was employed to investigate the size and morphology of the polymers. The specific surface area of the polymers was determined by Brunauer-Emmett-Teller (BET) analysis through performing nitrogen adsorption experiments, and the measurement was operated on AUTOSORB 1 (Quantachrome Instruments, Germany), and the polymers were degassed in vacuum at 300 °C prior to adsorption measurements. Zeta potential measurements were performed on a Malvern Zetasizer Nano-ZS90 (ZEN3590, UK).

2.3. Preparation of Hg-IIPs

Hg-IIPs based on dithzone-Hg^{2+} interactions were prepared by sol–gel process similar to a reported procedure[33] with necessary modification, as follows. Dithzone (256 mg) and $HgCl_2$ (108 mg) were dissolved in a 100 mL ethanol to form a complex as template molecules, followed by adding APTES (467 μL) as function monomers, which were stored at 4 °C in dark for 6 h. Then, TEOS (2 mL) as crosslinking agent and aqueous ammonia (5 mL, 14%) were added in the mixing solution. The polymerization reaction was undertaken with magnetic stirring at room temperature for 12 h, and the product was further aged by stirring at 60 °C for 6 h to obtain high cross-linking density and interconnected macroporous structures. The resultant IIPs were obtained by centrifugation and rinsing with anhydrous ethanol for three times to wash off the residues. Hg^{2+} was removed from the prepared IIPs by several sequential elution steps with 0.5 mol/L HCl under vigorous stirring. The final products were washed with DDI water up to pH 6–7 and were dried under vacuum at 40 °C. For simplicity, the obtained polymers were named Hg-IIPs. For comparison, the non-imprinted polymers (NIPs) as control materials were prepared using the same procedure and conditions, only in the absence of template molecules.

2.4. Batch procedure

To evaluate ion recognition properties of the Hg-IIPs, solution pH effect, static and dynamic adsorption, selectivity and reusability were tested by a batch procedure method. The procedures were carried out as follows. The Hg-IIPs (20 mg) were equilibrated with 10 mL of aqueous solutions containing 20 mg/L Hg^{2+} with pH varying from 2 to 9 (adjusted using 0.1 mol/L phosphate buffer) at room temperature for 12 h. The pH was maintained in a range of ±0.1 units, the tested solutions were centrifuged and the supernatant solutions were collected, which was filtrated through a 0.45 μm membrane, and then the filtrate solutions were determined by AFS. The instrumental response was periodically checked with known metal standard solutions. The experiments were performed in triplicates.

Static adsorption was examined using 10 mL aqueous solutions containing Hg^{2+} at various concentrations from 2 to 20 mg/L, incubating for 12 h under optimal sorption conditions. The binding amount (Q) of Hg^{2+} was calculated by subtracting the free concentrations from the initial concentrations. In a meanwhile, dynamic adsorption test was carried out by monitoring the temporal amount of Hg^{2+} in the solutions with the initial concentration of 10 mg/L. The mixture was continuously shaken in a thermostatically controlled water bath at room temperature for 0 to 160 min; the polymers were removed centrifugally. And the supernatant solutions were collected and determined using AFS, which was similar to that of the static adsorption test.

Selectivity adsorption experiments were studied by using Zn^{2+}, Cd^{2+}, Pb^{2+}, $MeHg^{+}$ and $EtHg^{+}$ with respect to the same concentration as Hg^{2+} (4 mg/L), which were treated with the Hg-IIPs and NIPs, respectively. And the supernatant solutions were collected and then determined using ICP-MS. Interference tests were investigated by using $MeHg^{+}$, $EtHg^{+}$, Na^{+}, K^{+}, Zn^{2+},Cu^{2+}, Pb^{2+}, Mg^{2+}, Ca^{2+}, Mg^{2+}, Cd^{2+} and Fe^{3+}, respectively, as co-existent ions individual at the concentration of 10 times of Hg^{2+} (40 mg/L). The experimental processes were similar to the above static adsorption test with the same polymer mass of 20 mg. All the tests were performed in triplicates. The average data from triplicate independent results were used for the following discussion.

In addition, the recognition ability of the Hg-IIPs was evaluated by using imprinting factor (α), which is defined as the following formula:

$$\alpha = Q_{\mathrm{IIP}} / Q_{\mathrm{NIP}} \qquad (1)$$

where, Q_{IIP} and Q_{NIP} are the adsorption amounts of template or analogues on IIPs and NIPs at equilibrium, respectively.

The reusability of Hg-IIPs was assessed by the adsorption–desorption experiments. Briefly, the Hg-IIPs were firstly put in Hg^{2+} solution (4 mg/L) for saturated adsorption, and then the adsorbed Hg^{2+} ions could be desorbed from the Hg-IIPs by treatment using 0.5 mol/L HCl as desorption medium, after being vigorously stirred for 2 h at room temperature; the final Hg^{2+} in the aqueous solution was detected by AFS. The adsorption–desorption studies were repeated ten times by using the same imprinted polymers.

2.5. Standard solution and practical sample preparation

The stock standard solutions of $MeHg^{+}$ at 1000 mg/L were obtained by dissolving appropriate amounts of methylmercury chloride in HPLC grade methanol. Lake water samples were collected into a teflon bottle from an artificial lake located in Laishan District of Yantai City. Surface seawater samples were collected into a teflon bottle from the Fisheman's Wharf of the Yellow Sea located in the coastal zone area of Yantai City. And the water samples were all filtrated through 0.45 μm PTFE syringe filters (Phenomenex, Los Angeles, CA, USA) to remove the suspended particles. The resultant filtrates which were directly analyzed or were alkalified to pH 7.0 using 0.1 mol/L NaOH, were kept in a refrigerator at 4 °C before use.

Two certified reference materials (CRMs), namely freeze-dried fish powder (BCR-463) and human hair (GBW07601(GSH-1)), purchased from the CRM/RM Information Center of China (Beijing, China), were used to validate the accuracy and the precision of the developed method. Moreover, for practical sample test, human hair samples were randomly collected from healthy volunteer subjects in our lab and fish meat was purchased from a local supermarket. They were treated according to that previously reported,[42] as follows. 1.0 g samples were added to a centrifuge tube containing 1.4 mL of 10 mol/L NaOH. The tube was heated at 90–95 °C for 30 min. Then the solution was cooled to room temperature and its pH value was adjusted to 7.0 using concentrated hydrochloric acid, followed by centrifugation for the supernatant. The treatment procedure was repeated three times. And all the three portions of supernatants were merged for AFS detection.

2.6. SPE procedure

A PTFE column (Phenomenex, Los Angeles, CA, USA) was packed with 200 mg of Hg-IIPs using a syringe with 4.0 mm i.d. The column was preconditioned successively with 5 mL of 0.1 mol/L HCl, 5 mL of DDI water and 5 mL blank solutions (standard or sample solutions without spiking). Then, 50 mL of sample solution containing Hg^{2+} at three concentrations (2, 5 and 10 μg/L) was passed through the column at a flow rate of 1.0 mL/min. The column was washed with 10 mL of DDI water and the adsorbed Hg^{2+} was eluted with 2.5 mL of 0.5 mol/L HCl, and then the extractants were detected by AFS. Each concentration was analysed by three replicates.

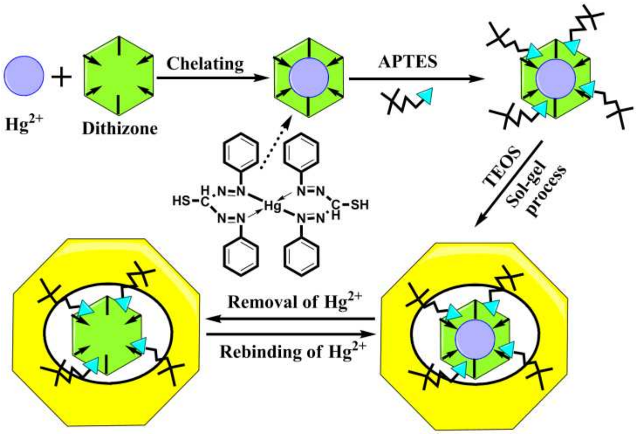

Fig. 1 Schematic illustration for preparation and imprinting process of Hg-IIPs.

3. Results and discussion

3.1. Preparation of Hg^{2+} imprinted IIPs

The synthesis and imprinting process of Hg^{2+} imprinted IIPs *via* sol–gel process is schematically shown in Fig. 1. First, the complex of Hg^{2+} and dithzone was produced based on the strong chelation of dithzone to Hg^{2+} ions, which was used as template molecules. The template molecules could easily pre-polymerize with the functional monomers APTES by non-covalent interactions. APTES, commonly used silane coupling agent for sol–gel process, was employed owing to the hydrophobic interaction. Then, the polymerizable group of APTES copolymerized with TEOS. Therefore, APTES played an important role in the preparation of Hg-IIPs. Finally, Hg^{2+} was removed by elution, leaving behind specific recognition sites on the surface of the polymers, with functional groups in a predetermined orientation and the proper size cavities exactly for Hg^{2+} ions, which would contribute to a high adsorption efficiency and selectivity for Hg^{2+} ions due to metal-ligand chemistry.[43]

Meanwhile, the adopted sol–gel process, with distinct characteristics such as easy fabrication, using ecofriendly reaction solvents, and mild polymerization conditions,[33] allowed dithizone–Hg^{2+} chelate as template to be readily embedded in the highly cross-linked host structure without the problem of thermal or chemical decomposition.

Moreover, it was found that dithizone chelated Hg^{2+} but not organic mercury compounds (Fig. S1). So, it is possible to realize the speciation analysis of mercury species using the Hg-IIPs based on the specific, strong chelation of dithzone. Meanwhile, AFS can only measure total mercury with the mercury hollow cathode lamp, without discriminating mercury species. Therefore, the prepared Hg-IIPs coupled with AFS would not only provide a superior selectivity for Hg^{2+}, but also possible speciation analysis.

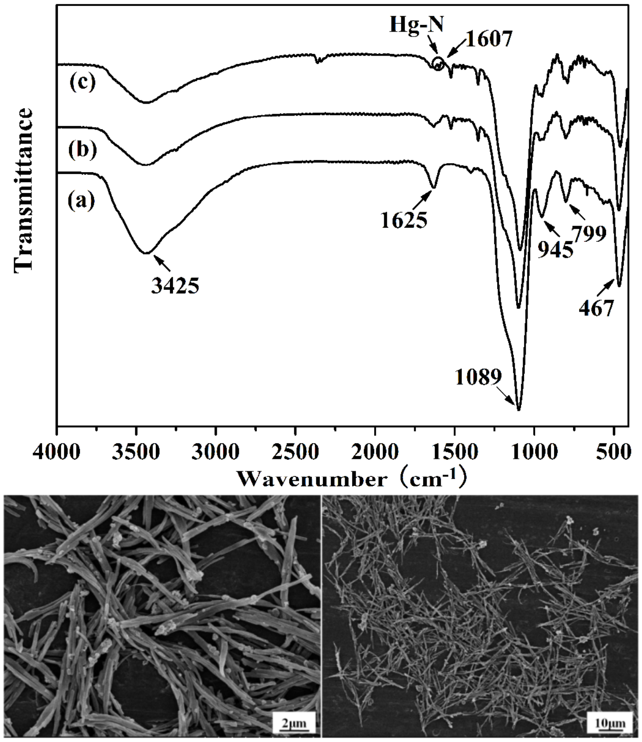

Fig. 2 (Upper) FT-IR spectra of (a) Hg-NIPs, (b) Hg-IIPs and (c) Hg contained Hg-IIPs. (Below) SEM images of Hg-IIPs.

3.2. Characterization of the Hg-IIPs

To confirm the presence of dithzone in the silica gel sorbents and its chelation for imprinting, the IR spectra of IIPs, Hg-contained IIPs and NIPs, were measured. As shown in Fig. 2 (upper), the wide and strong absorption band around 1089 and 945 cm^{-1} could be attributed to Si-O-Si and Si-O-H stretching vibrations, respectively, and the absorption peaks around 799 and 467 cm^{-1} belonged to Si-O vibrations, indicating the occurrence of silica matrices in the three materials. The strong and broad absorption band observed at 3425 cm^{-1} could be assigned to the N-H stretching vibration of APTES. Compared with NIPs, the characteristic absorption peak at 1625 cm^{-1} (Fig. 2a), most probably ascribed to the stretching vibrations of N=N double bonds of pyridine ring in dithzone, became weak significantly in the IIPs (Fig. 2b) and Hg-contained IIPs (Fig. 2c). Interestingly, a new peak appeared at 1607 cm^{-1} in Fig. 2c, which was just the characteristic of Hg-N bond. These observations demonstrated the coordination of dithzone through the N atom from its fragment, indicating the metal-ligand bond had been formed between Hg^{2+} and chelating groups in IIPs. The FT-IR results confirmed the Hg-IIPs were successfully prepared based on the metal–ligand chemistry by sol–gel polymerization.

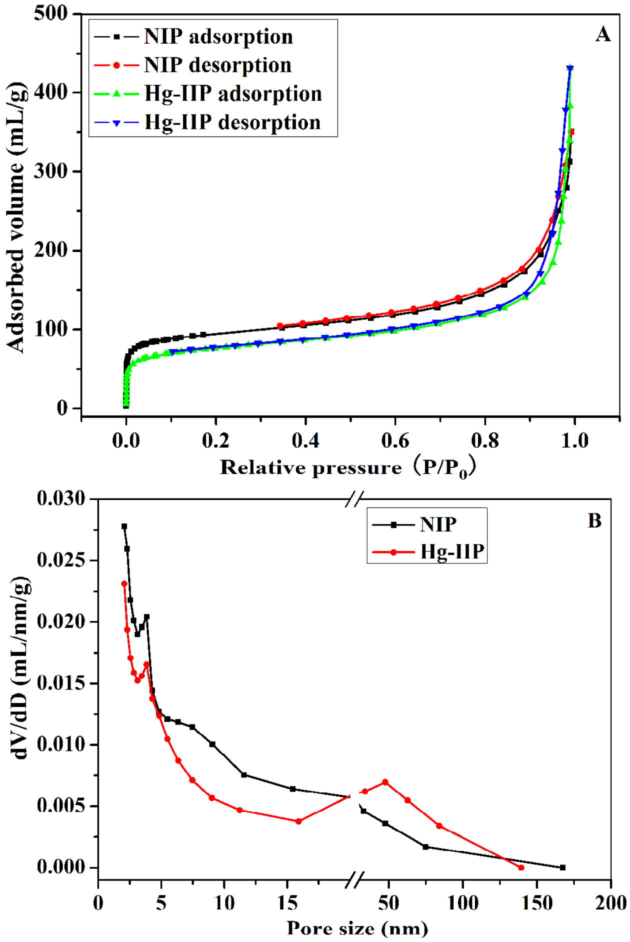

Fig. 3 (A) N_2 adsorption-desorption isotherms and (B) pore size distribution of IIPs and NIPs.

SEM images were supplied to characterize the surface morphologies of the Hg-IIPs. As observed, the IIPs displayed a dendritic structure, and seemed to be covered with particles in several areas (Fig. 2, below). The particles were very likely to be the aggregated silicon particles owing to the use of APTES in the sol–gel process. Because the imprinting polymerization process occurred, the polymers demonstrated a dendritic structure. However, in the absence of imprinting process, silicon particles aggregation materials could easily be formed. So, herein, the dendritic-structured IIPs were reasonable with part coverage of aggregated silicon particles. In addition, by BET analysis, the specific surface area of Hg-IIPs was attained of 43.27 m^2/g higher than that of corresponding NIPs (22.92 m^2/g). Fig. 3A shows N_2 adsorption-desorption isotherms of the Hg-IIPs and corresponding NIPs. As seen, when the relative pressure P/P_0 was less than 0.8, the slope of the curves was very small, indicating that very little amount of small size pores were present on the surface of IIPs. However, when the relative pressure P/P_0 was higher than 0.8, the slope of the curves significantly increased. As seen, the desorption curve was closer but leveled slightly above the adsorption curve, which could be the evidence of a small quantity of micropores existing on the IIPs.[44] As shown from Fig. 3B, the average pore size of IIPs and NIPs were 9.42 and 5.62 nm, respectively. The narrow pore diameter distribution and low average pore diameter suggested that the size of the cavities formed in the IIPs played a key role in binding capacity. Related morphological structure parameters of IIPs and NIPs were listed in Table S1. As seen, the results indicated the IIPs had uniform regular structure. The large cumulative pore volume was very likely owing to the microspores on the surface of IIPs, which revealed that the Hg^{2+} ions were almost completely eluted and removed and thereby leading to considerable amounts of imprinting cavity sites.

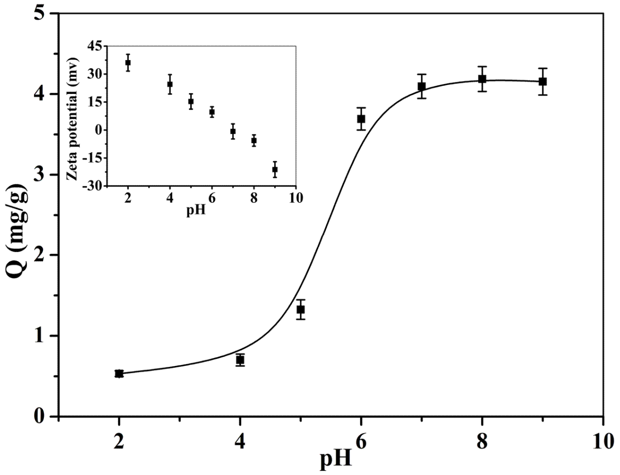

Fig. 4 Effect of pH on adsorption of Hg^{2+} for Hg-IIPs. (Inset) Effect of pH on Zeta potential of Hg-IIPs. Experimental conditions: IIPs, 20 mg; C_0, 10 mg/L; V, 10 mL; adsorption time, 12 h.

3.3. Binding properties of the IIPs for Hg^{2+}

Solution acidity plays an important role in the adsorption capacity because it generally affects the complexing reaction between metal ions and ligands. In order to evaluate the effect of varying pH on Hg^{2+} adsorption, a batch procedure was used. As seen from Fig. 4, the adsorption capacity was very low at pH values below 4.0. The N atoms of dithizone are highly protonated at low pH, and the electronic-supply ability of N atoms will be significantly weaken and thereby reducing the chelating of dithizone for Hg^{2+} ions,[31,32] which in turn will reduce the adsorption capacity of Hg-IIPs. Along with the increase of pH within 4–6, the adsorption capacity increased rapidly, because the protonation ability of N atoms of dithizone became weak and thereafter enhanced adsorption capacity of dithizone for Hg^{2+}. After pH 6.0, the increase was relatively slow and the adsorption capacity approached the maximum at pH 8.0. However, at pH>9, the formation and precipitation of metal hydroxide, as well as quick decomposition, will easily occur. At the same time, the IIPs would change into electronegative, resulting in adsorbing various metal ions to a certain extent, and thus cause the loss of selectivity. In addition, as can be seen from the inset of Fig. 4, Zeta potential of Hg-IIPs varied in different pH values with an excellent linearity in a range of pH 2–9. So, the adsorption capacity of IIPs for Hg^{2+} was dependent on pH values. The optimum pH for adsorption of Hg^{2+} from aqueous solutions ranged from 7.0 to 8.0. And within this range, neither precipitation of the metal hydroxide nor the protonation of the N atoms occurred obviously. Combining the consideration of physiological conditions, therefore, pH 7.0 was selected as optimum for further experiments.

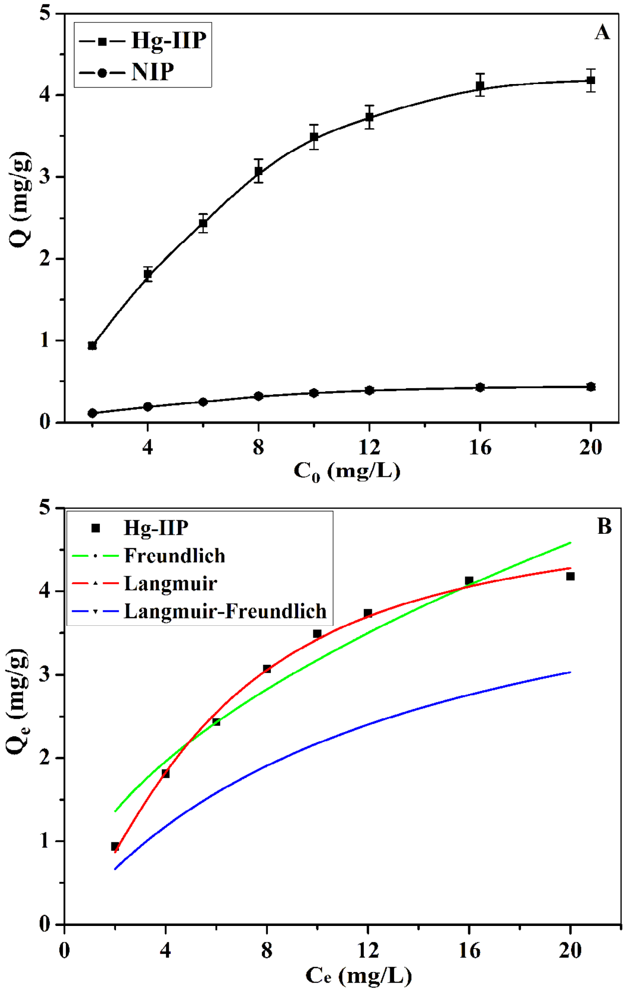

Fig. 5 (A) Static adsorption isotherm curves of IIPs and NIPs for Hg^{2+} in aqueous solutions, and (B) comparision of Langmuir, Freundlich and Langmuir-Freundlich isotherm models for Hg^{2+} adsorption process onto the IIPs. Experimental conditions: V, 10 mL, polymer, 20 mg, adsorption time, 12 h, room temperature.

Then static adsorption experiments were investigated in order to evaluate the adsorption capacities of Hg-IIPs for the Hg^{2+} within 2–20 mg/L with pH 7.0. As can be seen from Fig. 5A, the amounts of Hg^{2+} adsorbed per unit mass of IIPs increased with the increase of initial concentrations of Hg^{2+}, and then began to level off after 16 mg/L. Excitingly, the experimentally obtained maximum adsorption capacity of Hg-IIPs was about 10 times of NIPs, presenting the imprinting factor *α* of 9.58. So, it suggested the IIPs possessed high imprinting effect owing to the high binding affinity for Hg^{2+}. Furthermore, the obtained static capacity data for IIPs were fitted using Langmuir, Freundlich and Langmuir-Freundlich isotherm models. As shown in Fig. 5B, the Langmuir isotherm model yielded the best fit, for the highest correlation coefficient of R^2=0.998 (Table S2). So, the data obtained from the equilibrium studies of the adsorption of Hg^{2+} ions onto Hg-IIPs may follow the Langmuir model, which assumes that the adsorption occurs at specific homogeneous sites on the adsorbent and can be successfully applied to monolayer adsorption processes.[45] It indicated that Hg^{2+} ions were adsorbed as a monolayer onto the surface of Hg-IIPs. Additionally, the highest concentration of binding sites per gram of polymers and the largest median binding affinity (Table S2), further conforming the excellent imprinting effect due to a number of specific binding sites on the Hg-IIPs.

Dynamic binding experiments were carried out to evaluate the binding rate and ion transfer property of Hg^{2+} onto the IIPs. As can be seen from Fig. S2A, a time of 80 min was needed to reach adsorption equilibrium for Hg-IIPs; in the same adsorption time, the binding capacity of Hg-IIPs was remarkably higher than that of NIPs, indicating the rebinding *via* metal-ligand bond was in favor of ion transfer and binding capacity. Furthermore, the dynamic binding was investigated by using different models including pseudo-first-order, pseudo-second-order, Elovich and intra-particle diffusion.[46] With the highest correlation coefficient of R^2=0.999 (Table S3), the pseudo-second-order model provided the most suitable correlation for the Hg-IIPs adsorption, which can be expressed as follows:

$$\frac{t}{Q_t} = \frac{1}{k_2 Q_e^{\ 2}} + \frac{t}{Q_e} \qquad (2)$$

where, Q_t means the instantaneous binding capacity at time t, Q_e is the equilibrium binding capacity, and k_2 is the rate constant. The obtained Q_e of 3.74 μmol/g calculated from the model was in good agreement with the Q_e of 3.68 μmol/g from experimental results. Also, as shown in Fig. S2B, the curve in the entire time period was found to be the better for predicting the kinetic process than other models. So, the adsorption could be deduced to follow the pseudo-second-order kinetics model. It could be supposed that the rate-limiting step might be chemisorption involving valency forces through sharing or exchange of electrons between sorbent and sorbate.[47] Therefore, the chemisorption could be the rate-limiting step in the adsorption process of IIPs for Hg^{2+}, further confirming the Hg-IIPs were prepared based on the metal–ligand chemistry.

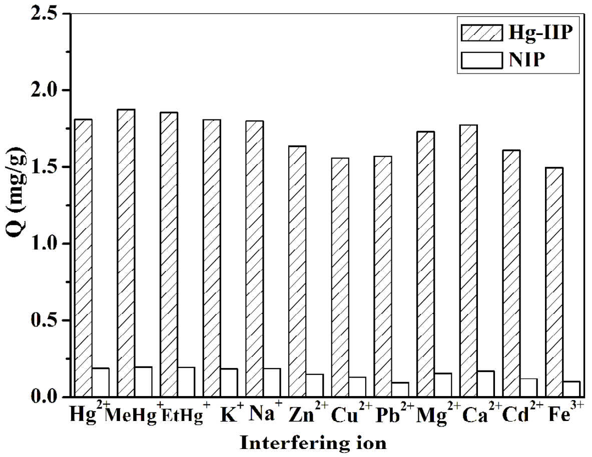

Fig. 6 Adsorption capacities for Hg^{2+} in the presence of 4 mg/L Hg^{2+} and 40 mg/L other metal ions, including $MeHg^+$, $EtHg^+$, Na^+, K^+, Zn^{2+}, Cu^{2+}, Pb^{2+}, Mg^{2+}, Ca^{2+}, Mg^{2+}, Cd^{2+} and Fe^{3+}, respectively. Experimental conditions: IIPs, 20 mg; V, 10 mL; sample solution, pH 7.0.

3.4. Ionic selectivity and recognition reliability of the IIPs

High ionic selectivity and recognition reliability is recognized the chief requirement and feature of IIPs. Competitive adsorption from the binary mixtures including $Hg^{2+}/MeHg^+$, $Hg^{2+}/EtHg^+$, Hg^{2+}/Zn^{2+}, Hg^{2+}/Cd^{2+} and Hg^{2+}/Pb^{2+} was investigated in selective binding experiments because these ions often coexisted in practical samples. As can be seen in Table 1, the competitive adsorption capacity of Hg-IIPs for Hg^{2+} is much higher than NIPs. The selective coefficients of Hg-IIPs for the binary mixtures were attained of 19–34, which is very likely owing to the highly selective Hg^{2+}-dithizone interactions. Moreover, interestingly, it implied that the determination of organic mercury can be realized using the IIPs, by subtracting the amounts of Hg^{2+} from total mercury.

Table 1 Selectivity of the prepared Hg-IIPs and NIPs.

Metal ions	Hg-IIPs		NIPs	
	D^a (mL/g)	S^b	D (mL/g)	S
Hg^{2+}	452.8	–	47.3	–
$MeHg^+$	23.8	19.06	28.1	1.67
$EtHg^+$	21.1	21.56	26.2	1.82
Zn^{2+}	13.5	33.54	15.3	3.10
Cd^{2+}	16.9	26.63	21.8	2.17
Pb^{2+}	20.5	22.09	23.3	2.03

[a] Distribution ratio, *D=Q/Ce.*

[b] Selective coefficient, $S = D_{template}/D_{competetive\ ion}$. $D_{template}$ and $D_{competetive\ ion}$ are distribution ratio of the template and the competitive ions on IIPs or NIPs, respectively.

In order to further evaluate the anti-interference ability and reliability of the IIPs for Hg^{2+}, the mixture solutions containing Hg^{2+} and various possible interfering ions with separate presence individual at 10 times excess, were examined. As shown in Fig. 6, those ions did not cause significant interference without remarkable capacity reduction for Hg^{2+} determination after the IIPs preconcentration procedure, and it could be estimated that only <10% of binding sites were taken over by the 10 times interfering ions. All the results indicated that the Hg-IIPs were highly selective and reliable for Hg^{2+} recognition.

3.5. Reusability of the IIPs

As an important index, reusability of the IIPs is also investigated owing to its pivotal role in cost-saving. Desorption of Hg^{2+} from the IIPs were studied by using 0.5 mol/L HCl, and 0.5 mol/L HCl plus 0.1 mol/L thiourea, respectively. It was found that the rebinding capacity was significantly reduced when using the latter as desorption medium, which was very likely owing to that the non-covalent interaction between functional monomers and dithizone was disrupted and thereby the complex of dithzone and

Hg^{2+} was desorbed. In contrast, after treatment with 0.5 mol/L HCl alone, the IIPs displayed high rebinding capacity without obvious decrease. It could be inferred that the chelation of dithizone for Hg^{2+} was destroyed and Hg^{2+} ions were subsequently released into the desorption medium, which satisfied the concept and requirement of IIPs. So, 0.5 mol/L HCl as ideal desorption medium was utilized for the repeated 10 adsorption-desorption cycles. Finally, the Hg-IIPs still presented high rebinding capacities for Hg^{2+}, with only a slight decrease within 5%. Consequently, the Hg-IIPs occupied excellent reusability and regeneration ability, which is in favor of actual applications.

3.6. Analytical performances for Hg^{2+} and organic mercury determination by using IIPs-SPE

Based on the above results, accordingly the Hg-IIPs could be employed as SPE sorbents for preconcentration of Hg^{2+}. The analytical performances of Hg-IIPs-SPE coupled with AFS for Hg^{2+} and total Hg determination were investigated. Under the optimized SPE conditions, an excellent linearity from 0.05 to 15 μg/L for Hg^{2+} was presented, and the relative standard deviation (RSD) at 2 μg/L was 5.2%. The limit of detection (LOD) based on three times the standard deviation and for 10 replicate measurements of a blank solution, was attained of 0.015 μg/L, which was much lower than the mandated upper limit of 2 μg/L for Hg^{2+} in drinking water by United States Environmental Protection Agency (USEPA). This indicated that the Hg-IIPs-SPE-AFS potentially applicable for sensitive accurate determination of Hg^{2+} in drinking water.

Using the developed method, by virtue of minusing, the organic mercury species could be determined. The LOD for $MeHg^+$ was achieved of 0.02 μg/L, which was higher than the permitted maximum concentration level (MCL) of 0.001 μg/L by China. Nevertheless, in a sense, the method sensitivity might contribute to mercury speciation analysis in water samples especially industrial and sanitary wastewater. The LOD for $EtHg^+$ was 0.02 μg/L, and it was lower than the MCL of 0.1 μg/L formulated by China. In addition, the RSDs at 2 μg/L were in a range of 6–11%. Hence, the Hg-IIPs-SPE-AFS could recognize and detect organic mercury. Thus, this method was clearly proved potentially feasible to quantitatively analyze organic mercury in real water samples.

Table 2 Determination of $MeHg^+$ and total Hg in certified reference materials (CRMs).[a]

CRMs	Certified (μg/g)		Determined (μg/g)[b]		Determined (μg/g)[c]	
	$MeHg^+$	Total Hg	$MeHg^+$	Total Hg	$MeHg^+$	Total H
BCR-463	2.85±0.16	3.04±0.16	2.95±015[d]	3.21±0.15	2.89±0.14	3.15±014
GBW07601	–	0.36±0.08	ND[e]	0.38±0.07	ND	0.37±006

[a] The comparison of the developed Hg-IIPs-SPE-AFS and ICP-MS results was made by using the *t*-test at the 95% confidence level.
[b] Results obtained from this method using AFS.
[c] Results obtained by ICP-MS.
[d] Average value of three determinations ± standard deviation.
[e] Not detected.

In order to validate this established method, the Hg-IIP-SPE procedure was applied to the CRMs, BCR-463 (fish meet) and GBW07601 (human hair). As shown in Table 2, the determined values for MeHg and total Hg were 2.95±0.15 μg/g and 3.21±0.15 μg/g, respectively, in BCR-463, and for total Hg was 0.38±0.07 μg/g in GBW07601, which agreed well with the certified values. The *t*-test proved there was no significant difference between the developed method and the ICP-MS determination at the 95% confidence level. Therefore, the Hg-IIPs-SPE-AFS was proved accurate and reliable for mercury speciation analysis in real solid and semi-solid samples.

Table 3 Analytical results of determination of seawater and lake water samples spiked with Hg^{2+}.

Sample	Added (μg/L)	Found (μg/L)	Recovery[a]±RSD[b] (%)	ICP-MS results (μg/L)
Seawater	0	0.21	–	0.23
	2	2.15	97.0±5.3	2.05
	5	5.47	105.2±4.7	5.07
	10	9.76	95.5±3.2	9.84
Lake water	0	0.31	–	0.29
	2	2.24	95.5±4.5	2.06
	5	4.96	93.0±2.9	5.09
	10	10.74	104.4±3.6	10.13

[a] Average value from five individual experiments.
[b] Relative standard deviation.

3.7. Applications of the IIPs-SPE to environmental and biological samples

In order to evaluate the practical applicability of the developed method for the mercury speciation analysis, the IIPs-SPE was further applied for environmental water samples and biological samples. As shown in Table 3, recoveries were in the range of 93.0–105.2%, with the RSD of 2.9–5.3%, suggesting the obtained IIPs *via* the chelating interaction of dithzone and Hg^{2+} accompanied with dual functional monomers were ideal candidates for SPE sorbents, and were greatly applicable for the effective enrichment and quantitative determination of trace Hg^{2+} in real water samples. At the same time, it suggested matrix effects were sharply reduced after the IIPs-SPE procedure. Additionally, the *t*-test proved the determined data were good consistent with that obtained by ICP-MS (Table 3). Hence, the method was feasible for real sample analysis with a high accuracy and good reliability. Moreover, the endogenous contents of Hg^{2+} were detected at 0.21 and 0.31 μg/L in the tested seawater and lake water samples, respectively. The value is much lower than the permitted Hg^{2+} (2.0 μg/L) in drinking water by USEPA. So, the validated IIPs-SPE coupled to AFS method might well be an ideal alternative to simultaneous enrichment, separation and determination of Hg^{2+} in complicated water samples for environmental monitoring and remediation purpose.

Table 4 Analytical results of the determination of Hg^{2+}, $MeHg^+$ and $EtHg^+$ in biological samples.

Sample	Added (μg/L)			Found (μg/L)		Recovery±RSD (%)	
	$MeHg^+$	$EtHg^+$	Hg^{2+}	Organic mercury[a]	Total Hg	Organic mercury	Total Hg
Human hair	0	0	10	ND	9.85	–	98.5±2.4
	10	0	10	10.45[b]	21.23	104.5±8.1	106.2±4.2
	0	10	10	9.78	18.52	97.8±7.9	92.6±3.4
Fish meat	0	0	10	ND	10.24	–	102.4±4.1
	10	0	10	9.62	18.76	96.2±9.3	93.8±5.3
	0	10	10	9.78	19.75	97.8±8.6	98.8±3.7

[a] Organic mercury value was obtained by the total Hg value minusing Hg^{2+} value.

[b] Average value from three individual experiments.

Also, the practicality of the IIPs-SPE for organic mercury in biological samples was investigated. As observed in Table 4, the high recoveries for organic mercury ranged from 97.8–104.5% with RSDs of 7.9–8.1% and 96.2–97.8% with RSDs of 8.6–9.3% for human hair and fish meat samples, respectively. Therefore, the IIPs-SPE-AFS was demonstrated to be capable of simply, sensitively identifying and detecting organic mercury species.

3.8 Comparison with other methods

Method performance of this developed chelate imprinting strategy toward mercury species was compared with that of some reported IIPs-SPE based methods. As shown from Table S4, as a new material, the prepared IIPs are ideal sorbent candidates in SPE for preconcentration of Hg^{2+}. The attained LOD is lower than or comparable to that reported,[33,34,48] and the most species inlcuding Hg^{2+}, $MeHg^+$ and $EtHg^+$ are analysed. The presented IIPs are simpler and easier to prepare, using cheaper classic ligand (dithizone) than 1-pyrrolidinedithiocarboxylic acid[34] and diazoaminobenzene[48] by more mild sol–gel process, as well as avoiding synthesizing procedures.[33] Moreover, more samples are applicable involving environmental and biological samples.

4. Conclusions

In summary, the novel Hg^{2+} IIPs based on dithizone-Hg^{2+} chelation were successfully prepared and applied to environmental and biological samples for preconcentration of Hg^{2+} and thus mercury speciation analysis, by a facile sol–gel process. Using the complex of dithizone-Hg^{2+} as template, the easily obtained IIPs displayed fast adsorption kinetics and high binding capacity for Hg^{2+}, excellent selectivity towards Hg^{2+} over organic mercury and other metal ions, as well as high anti-interference ability for Hg^{2+} recognition and adsorption. Coupled to AFS detection, the high detection ability up to 0.015 μg/L for Hg^{2+} and 0.02 μg/L for organic mercury could be achieved, comparable to or even surpassing that afforded by traditional chromatography-mass spectroscopy methods. The method accuracy was validated with very consistent results for CRMs. Also, the practical applicability was demonstrated for the analysis of Hg^{2+} in seawater and lake water samples, together with organic mercury species in human hair and fish meat samples. Therefore, the IIPs-SPE-AFS proved a very promising sensitive, simple and ecofriendly alternative to the classical methods for the mercury speciation analysis in aqueous, solid and semi-solid environmental and biological samples.

On the other hand, by means of the model of Hg^{2+} imprinting, we purpose to develop a simple general applicable IIPs based platform for heavy metal ions and species. For example, $MeHg^+$ also can be imprinted by using specific ligands and/or functional monomers. With the suitable choice and reasonable utilization of chelation and traditional ligands and functional monomers especially commercially available, furthermore, by smartly devising and synthesizing new ligands and functional monomers, the IIPs-based heavy metal detection/removal platform can be constructed and developed for selective sensitive routine monitoring/remediation of environmental and biological samples. Such an excellent platform has great potential for imprinting various heavy metals, which certainly will greatly push forward the development of heavy metal speciation analysis and enrich the research connotations of molecular imprinting technologies. We believe that it will provide new opportunities to explore novel IIPs/MIPs for potential utilizations. Our efforts along this aspect are currently underway.

Acknowledgements

This work was financially supported by the National Natural Science Foundation of China (21275158, 21105117, 21107057, 21275068), the Scientific Research Foundation for the Returned Overseas Chinese Scholars, State Education Ministry, and the Innovation Projects of the Chinese Academy of Sciences (KZCX2-EW-206).

[a] *Key Laboratory of Coastal Environmental Processes and Ecological Remediation, Shandong Provincial Key Laboratory of Coastal Environmental Processes, Yantai Institute of Coastal Zone Research, Chinese Academy of Sciences, Yantai 264003, China*
[b] *School of Chemistry & Chemical Engineering, Linyi University, Linyi 276005, China*
[c] *Key Lab of Environmental Engineering in Shandong Province, School of Environment & Municipal Engineering, Qingdao Technological University, Qingdao 266033, China*
[d] *University of Chinese Academy of Sciences, Beijing 100049, China*
** Corresponding author. Tel/Fax: +86 535 2109130.*
E-mail address: lxchen@yic.ac.cn (L. Chen).

Supporting information

The UV-vis spectra of dithizone alone and the dithizone with mercury species, the adsorption kinetics curves of Hg-IIPs/NIPs for Hg^{2+} and kinetics models data, the specific surface area and other related data of Hg-IIPs/NIPs obtained by BET, the isotherm model parameters for Hg-IIPs/NIPs, and the parameters obtained of Hg^{2+} adsorption towards Hg-IIP from four kinetic models. This information is available free of charge via the Internet at http://pubs.acs.org/.

Notes and references

1 Q. H. Wu, N. F. Y. Tam, J. Y. S. Leung, X. Z. Zhou, J. Fu, B. Yao, X. X. Huang and L. H. Xia, *Ecotox. Environ. Safe.*, 2014, **104**, 143.
2 G. Aragay, J. Pons and A. Merkoc, *Chem. Rev.*, 2011, **111**, 3433.
3 A. R. Timerbaev, *Chem. Rev.*, 2013, **113**, 778.
4 Y. G. Yin, J. F. Liu and G. B. Jiang, *Chin. Sci. Bull.*, 2013, **58**,150.
5 Z. F. Liu, Z. L. Zhu, H. T. Zheng and S. H. Hu, *Anal. Chem.*, 2012, **84**, 10170.
6 J. H. Li, W. H. Lu, J. P. Ma and L. X. Chen, *Microchim. Acta*, 2011, **175**, 301.
7 L. H. Reyes, G. M. Mizanur Rahman, T. Fahrenholz and H. M. Kingston, *Anal. Bioanal. Chem.*, 2008, **390**, 2123.
8 F. A. Duarte, B. M. Soares, A. A. Vieira, E. R. Pereira, J. V. Maciel, S. S. Caldas and E. G. Primel, *Anal. Chem.*, 2013, **85**, 5015.

9 J. B. Shi, L. N. Liang, G. B. Jiang and X. L. Jin, *Environ. Int.*, 2005, **31**, 357.
10 D. Karunasagar, M. V. Balarama Krishna, S. V. Rao and J. Arunachalam, *J. Hazard. Mater.*, 2005, **118**, 133.
11 F. F. Yang, J. H. Li, W. H. Lu, Y. Y. Wen, X. Q. Cai, J. M. You, J. P. Ma, Y. J. Ding and L. X. Chen, *Electrophoresis*, 2014, **35**, 474.
12 D. Yan, L. M. Yang and Q. Q. Wang, *Anal. Chem.*, 2008, **80**, 6104.
13 Y. Li, Y. Jiang and X. P. Yan, *Anal. Chem.*, 2006, **78**, 6115.
14 T. Yordanova, I. Dakova, K. Balashev and I. Karadjova, *Microchem. J.*, 2014, **113**, 42.
15 J. Margetínová, P. H. Pelcová and V. Kubáñ, *Anal. Chim. Acta*, 2008, **615**, 115.
16 W. B. Zhang, X. A. Yang, Y. P. Dong and J. J. Xue, *Anal. Chem.*, 2012, **84**, 9199.
17 Y. Y. Wen, J. H. Li, J. P. Ma and L. X. Chen, *Electrophoresis*, 2012, **33**, 2933.
18 W. A. W. Ibrahim, L. I. Abd Ali, A. Sulaiman, M. M. Sanagi and H. Y. Aboul-Enein, *Anal. Chem.*, 2014, **44**, 233.
19 Y. Y. Wen, L. Chen, J. H. Li, D. Y. Liu, L. X. Chen, *TRAC-Trend. Anal. Chem.*, 2014, **59**, 26.
20 L. X. Chen, S. F. Xu and J. H. Li, *Chem. Soc. Rev.*, 2011, **40**, 2922.
21 X. Q. Cai, J. H. Li, Z. Zhang, F. F. Yang, R. C. Dong and L. X. Chen, *ACS Appl. Mater. Interfaces*, 2014, **6**, 305.
22 N.T. Hoai, D. K. Yoo, D. Kim, *J. Hazard. Mater.*, 2010, **173**, 462.
23 C. R. T. Tarley, F. N. Andradea, F. M. Oliveirac, M. Z. Corazzac, L. F. M. Azevedoa and M. G. Segatelli, *Anal. Chim. Acta,* 2011, **703**,145.
24 S. L. Wei, Y. Liu, M. D. Shao, L. Liu, H. W. Wang and Y. Q. Liu, *RSC Adv.*, 2014, **4**, 29715.
25 N. Zhang and B. Hu, *Anal. Chim. Acta,* 2012, **723**, 54.
26 A. Bhaskarapillai and S. V. Narasimhan, *RSC Adv.*, 2013, **3**, 13178.
27 B. B. Prasad, D. Jauhari and A. Verma, *Talanta*, 2014, **20**, 398.
28 C. Branger, W. Meouche and A. Margaillan, *React. Func. Polym.*, 2013, **73**, 859.
29 C. R. Preetha, J. M. G. Ladis and T. P. Rao, *Environ. Sci. Technol.*, 2006, **40**, 3070.
30 T. Alizadeh, M. R. Ganjali and M. Zare, *Anal. Chim. Acta*, 2011, **689**, 52.
31 B. BaliPrasad, D. Jauhari and A. A. Verma, *Talanta*, 2014, **120**, 398.
32 S. Clemens, M. Monperrus, O. F. X.Donard, D. Amouroux and T. Guerin, *Talanta*, 2012, **89**, 12.
33 S. F. Xu, L. X. Chen, J. H. Li, Y. F. Guan and H. Z. Lu, *J. Hazard. Mater.*, 2012, **237–238**, 347.
34 I. Dakova, T. Yordanova and I. Karadjova, *J. Hazard. Mater.*, 2012, **231**, 49.
35 J. Tan, H. F. Wang and X. P. Yan, *Biosens. Bioelectron.*, 2009, **24**, 3316.
36 K. Leopold, M. Foulkes and P. Worsfold, *Anal. Chim. Acta*, 2010, **663**, 127.
37 Y. G. Yin, M. Chen, J. F. Peng, J. F. Liu and G. B. Jiang, *Talanta*, 2010, **81**, 1788.
38 Z. A. Chandio, F. N. Talpur, H. Khan, H. I. Afridi, G. Q. Khaskheli and M. A. Mughal, *RSC Adv.*, 2014, **4**, 3326.
39 X. L. Song, J. H. Li, S. F. Xu, R. J. Ying, J. P. Ma, C. Y. Liao, D. Y. Liu, J. B. Yu and L. X. Chen, *Talanta*, 2012, **99**, 75.
40 H. He, D. L. Xiao, J. He, H. Li, H. He, H. Dai and J. Peng, *Analyst*, 2014, **139**, 2459.
41 J. E. Lofgreen and G. A. Ozin, *Chem. Soc. Rev.*, 2014, **43**, 911.
42 Y. W. Liu, Y. H. Zai, X. J. Chang, Y. Guo, S. M. Meng and F. Feng, *Anal. Chim. Acta*, 2006, **575**, 159.
43 J. J. Becker and M. R. Gagnea, *Acc. Chem. Res.*, 2004, **37**, 798.
44 X. Y. Wang, Q.Kang, D. Z. Shen, Z. Zhang, J. H. Li and L. X. Chen, *Talanta*, 2014, **124**, 7.
45 C. Herdes and L. Sarkisov, *Langmuir*, 2009, **25**, 5352.
46 J. H. Zhu, S. Y. Wei, H. B. Gu, S. B. Rapole, Q. Wang, Z. P. Luo, N. Haldolaarachchige, D. P. Young and Z. H. Guo, *Environ. Sci. Technol.*, 2012, **46**, 977.
47 Y. S. Ho and G. McKay, *Process Biochem.*, 1999, **34**, 451.
48 Y. W. Liu, X. J. Chang, D. Yang, Y. Guo and S. M. Meng, *Anal. Chim. Acta*, 2005, **538**, 85.